

# Dissolution of Barium Sulfate Scale Deposits by Chelating Agents

KAI DUNN AND TEH FU YEN\*

Department of Civil and Environmental Engineering,  
University of Southern California,  
Los Angeles, California 09989-2531

The occurrence of barium sulfate scale ( $\text{BaSO}_4$ ) is a severe problem and its associated environmental concerns in oil and gas production worldwide will cause considerable production losses. Chemical dissolution will create a new direction for controlling the scale deposits by chelating agents, which form strong complexes with metal ions in solution. Chemical dissolvers based on the aminoacetate group can be considered strong chelating agents for barium ions. Diethylenetrinitriropentaacetic acid (DTPA) and ethylenedinitrilotetraacetic acid (EDTA) are two major chelating agents used for the dissolution experiments. The kinetic studies for the dissolution reaction of scale-forming materials will be presented. Dissolution follows the first-order kinetics for the stirred system. The activation energies obtained in the stirred system of DTPA and EDTA, 9.59 and 9.31 kcal/mol, respectively, suggested that mass transfer is not the controlling factor. In this system, the surface reaction is considered as the rate-controlling step in the dissolution process. This study includes the dissolution kinetics in the aqueous system and surface phenomena on the solid. Surface phenomena such as morphology and surface pitting have been investigated by scanning electron microscopy. The morphology changes as a function of dissolution time.

## Introduction

The formation and deposition of mineral scales in oil reservoirs have long been major impediments to oil and gas production. During oil recovery from offshore oil-bearing reservoirs, pressure is maintained by injecting the well with seawater. A common problem with this procedure is that the formation water in the reservoir often contains high concentrations of alkaline-earth metal ions ( $\text{Ba}^{2+}$ ,  $\text{Ca}^{2+}$ , and  $\text{Sr}^{2+}$ ). When injected seawater, which contains sulfate ions ( $\text{SO}_4^{2-}$ ) comes into contact with the formation water in the region of the well bore, the resulting highly insoluble mineral scales block production tubing and also may affect the porosity of the reservoir (1–3). The scale typically consists of deposits of calcium carbonate (calcite), barium sulfate (barite), and sometimes a small amount of radioactive strontium sulfate. Barite is an extremely insoluble mineral (2.5 mg/L), which is important to the petroleum industry as a unique scaling agent.

Various studies have been done in the past for removing barium sulfate scale chemically. Most of these processes have utilized chelating or complexing agents (4–6). Polyaminodiacetic acid, such as diethylenetrinitriropentaacetic acid

(DTPA) and ethylenedinitrilotetraacetic acid (EDTA), can be used to dissolve the barium sulfate scale. Most dissolution studies have employed the solid particles stirred in water (7, 8) or with a chelating agent (4–6), with kinetic information inferred from changes in the chemical composition of the bulk solution, measured as a function of time. Many investigations have been reported on the kinetics of dissolution of mineral. These include studies of the dissolution of sulfate solids in water and sodium chloride brines (8), in acidified water (9), at various temperatures (10), with tracer study (11), and with chemical control (12). The influence of particle size on the dissolution has also been reported (4, 7). Microanalysis can be used to observe the surface phenomena undergoing initial dissolution. The scanning electron microscopy (SEM) observations (13–17) of barium sulfate crystal show the rhombohedral morphology on each single crystal. Some SEM examinations of barium sulfate undergoing dissolution have reported etch pits on the crystal surface (4, 17).

This work was to conduct experiments for the dissolution of barium sulfate scale by chelating agents. The dissolution rate constant and the empirical activation energy can be obtained through dissolution kinetics. For the study of surface phenomena, the microanalysis of scale surface examination will yield valuable information to support the dissolution mechanism and reaction modeling. It is expected that the optimum condition of dissolution can be implemented on field operation based on these fundamental investigations from designed experiments.

## Material and Methods

The barium sulfate samples used in this research were obtained from a production well at Chevron's Rangely field. The original samples were ground into tiny particles. The particles with size of 90–150  $\mu\text{m}$  (centered on 120  $\mu\text{m}$ ) were collected and washed by distilled water with sonication to remove fines before drying. After the particles were dried in an oven for about 5 min, these particles were ready for the dissolution experiment. The samples for the dissolution process were based on the assumption that the dissolved solid samples are of nearly the same particle size and shape. The specific surface area for this particle was calculated as 0.0105  $\text{m}^2/\text{g}$ .

The chelating agents based on the aminoacetate group formed effective scale dissolvers, such as DTPA and EDTA. The same concentration of 0.18 M for both dissolvers was used to test the scale dissolution. At a strong alkaline condition of pH above 12, the dissolvers were progressively deprotonated and became negative charges. Therefore, dissolvers at pH 12 used in dissolution tests could have strong affinity for barium ions.

Most of the dissolution experiments were carried out in a flask using 0.4 g of barium sulfate sample in 100 mL of 0.18 M dissolvers with a pH at 12. Three temperatures were used in the experiments: 40, 60, and 80 °C. Both different static and stirred modes were applied to the dissolution test. The best solution is for a stirred system, the experiments stood at test temperature with agitation by a fixed level using a magnetic stirrer. The stirring rate was kept constant in all experiments and was sufficient to ensure a smooth, non-turbulent circulation of the suspended barium sulfate particles. The assumption of the stirred system with a constant stirring rate is to eliminate the interference of transport on the surface for the dissolution process. Therefore,

\* To whom correspondence should be addressed. Phone: (213) 740-0586; fax: (213) 744-1426; e-mail: tfyen@mizar.usc.edu.

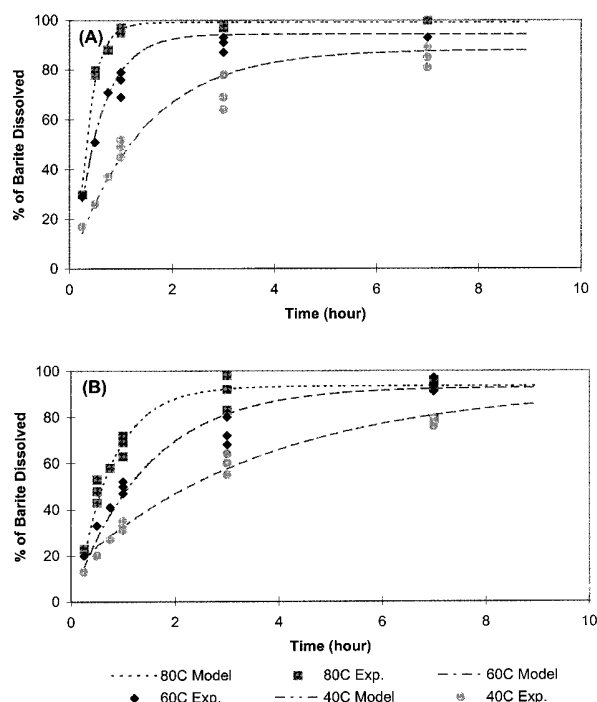


FIGURE 1. Barite dissolution profile curves by 0.18 M dissolvers in a stirred system: (A) DTPA, (B) EDTA.

the dissolution reaction under a stirred system can mostly depend on the surface reaction without much interference on mass transport. The chelation products of the dissolution test were analyzed by an inductively coupled plasma (ICP) analyzer from Bausch & Lomb ARL 3580.

Microanalysis can be used to observe the surface phenomena undergoing initial dissolution at ambient temperature. Scanning electron microscopy (SEM) was used to investigate the surface phenomena. The model of SEM is Cambridge 360. The mineral barium sulfate crystals were dissolved in a flask by 0.18 M DTPA or EDTA. The dissolution process could be terminated at a particular dissolution period. After the dissolution process, the solvent needs to be decanted from the flask, drying the particle for SEM examination. The morphology of crystal and the etch pits of crystal dissolution can be examined clearly by SEM.

## Results and Discussion

The barium sulfate dissolution test was accomplished in the experiment with a mild stirring condition to prevent diffusion interference on the surface of scale. In these tests, we determined the percentage of barium sulfate dissolved at multiple times (from several minutes to 1 day) to compare dissolver performance over an extended period of time. In Figure 1, barium sulfate dissolution tests are presented by 0.18 M dissolvers (DTPA in Figure 1A and EDTA in Figure 1B) in a stirred system. The results have demonstrated that the dissolution rate is strongly temperature dependent. The individual data are the raw experimental measurements; the dot-lines are the model fitting curves from the kinetics model.

**Kinetics Model.** On the basis of experimental results, a model of chemical reaction kinetics has been developed to analyze the experimental data of barite dissolution in a stirred system. The stoichiometric equation for an irreversible dissolution of barium sulfate scale by dissolver to form a complex can be described by a general reaction:



TABLE 1. Approximation of Rate Constant in a Stirred System

dissolver	$k_c(40^\circ\text{C}) (\text{h}^{-1})$	$k_c(60^\circ\text{C}) (\text{h}^{-1})$	$k_c(80^\circ\text{C}) (\text{h}^{-1})$
DTPA	0.711	1.985	4.068
EDTA	0.266	0.691	1.470

We have to make the following assumptions: (a) the ligands (L) are in great excess, (b) the rate of dissolution, expressed as the rate of increase of dissolved  $\text{Ba}^{2+}$  concentration in the solution, is first order to the mass concentration of  $\text{BaSO}_4(\text{s})$  remaining in the liquid suspension, and (c) eventually all  $\text{BaSO}_4(\text{s})$  dissolved (which is justified in the presence of excess ligands and irreversible reaction). Hence, the mass concentration of undissolved  $\text{BaSO}_4(\text{s})$  is proportional to  $C_\infty - C_t$ , where  $C_\infty$  is the ultimate concentration of  $\text{Ba}^{2+}$  and  $C_t$  is  $\text{Ba}^{2+}$  concentration at any instance, or

$$r_{\text{Ba}^{2+}} = k_c C_s = k_c (C_\infty - C_t)$$

$r_{\text{Ba}^{2+}}$  = reaction rate ( $\text{BaSO}_4$  dissolution)  
at steady state ( $\text{mol h}^{-1}$ )

$k_c$  = reaction rate constant ( $\text{h}^{-1}$ )

$C_s$  = mass concentration of  $\text{BaSO}_4(\text{s})$  remaining  
in the solution ( $\text{mg/L}$ )

$C_\infty$  = ultimate concentration of barium ( $\text{Ba}^{2+}$ )  
in solution ( $\text{mg/L}$ )

$C_t$  = concentration of barium ( $\text{Ba}^{2+}$ )  
in solution at time  $t$  ( $\text{mg/L}$ )

Since

$$r_{\text{Ba}^{2+}} = dC_t/dt$$

integration yields

$$\int_0^{C_t} \frac{dC_t}{C_\infty - C_t} = k_c \int_0^t dt$$

$$-\ln \frac{C_\infty - C_t}{C_\infty} = k_c t$$

or

$$\frac{C_\infty - C_t}{C_\infty} = \exp(-k_c t)$$

In this equation, the ultimate concentration  $C_\infty$  of  $\text{BaSO}_4$  in solution can be calculated before the dissolution experiment by assuming the  $\text{BaSO}_4$  solids are totally dissolved. Meanwhile, the barium concentration  $C_t$  indicates the amount of  $\text{BaSO}_4$  dissolved at time  $t$ . The model fitting curves in Figure 1A and 1B show the barite dissolution kinetics in a stirred system by DTPA and EDTA, respectively. The experimentally determined rate constants at different temperatures of barite dissolution in a stirred system are listed in Table 1.

**Activation Energy.** Table 1 lists three rate constants associated with different temperatures. The Arrhenius equation can be applied to the temperature effect on the experimental observations to find the activation energy. The activation energy for a chemical reaction is the minimum energy needed to initiate the reaction. A relation between the reaction rate and the magnitude of the activation energy

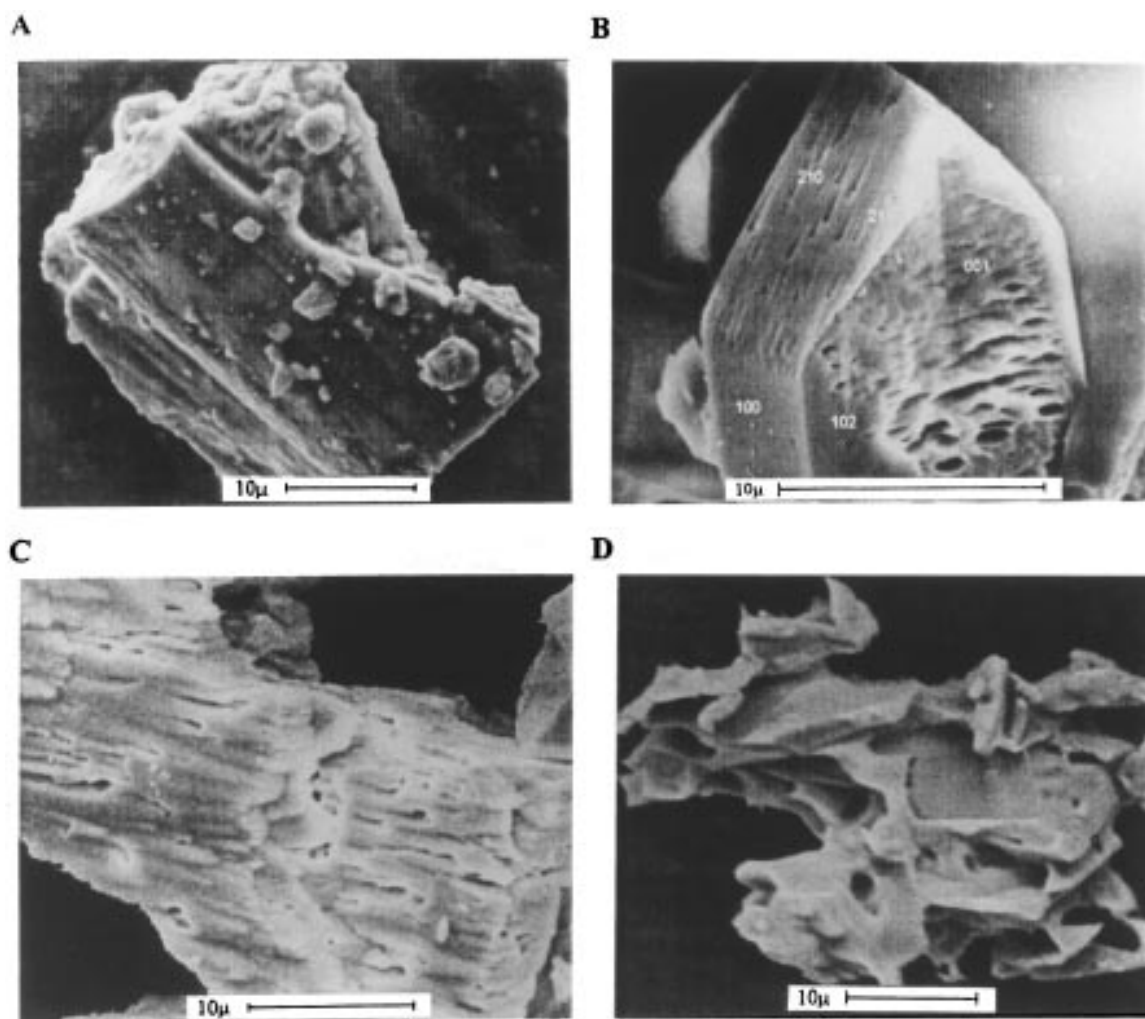


FIGURE 2. SEM investigations of barite dissolution by 0.18 M DTPA at 60 °C: (A) before dissolution process, (B) after 0.5 h dissolution, (C) after 1 h dissolution, (D) after 7 h dissolution. For detailed discussion of (B) to (D) see ref 26.

for different reactions occurring at the same temperature exists. From Arrhenius rate law:

$$k_c = A \exp\left(\frac{-E_a}{RT}\right)$$

$k_c$  = reaction rate constant ( $\text{h}^{-1}$ )

$A$  = frequency factor ( $\text{h}^{-1}$ )

$E_a$  = the energy of activation (kcal/mol)

$R$  = the ideal gas constant (1.987 cal/mol K)

$T$  = the temperature in K

A general trend of increasing rate with increasing temperature is perceivable. Arrhenius plots for the rate constants of Table 1 give activation energies of 9.59 kcal/mol ( $r^2 = 0.996$ ) for DTPA and 9.31 kcal/mol ( $r^2 = 0.999$ ) for EDTA. In Table 2, the activation energy,  $E_a$ , values reported in the literature on the dissolution and precipitation of barite are listed. The purpose of our studies was based on the industrial application for using chelating agents as dissolver solvents to treat scale problem in oil reservoir while the pH is fixed. Solvent properties are correlated with dissolution rate governed by solvation affinity for the near-surface divalent metals. There are some different properties between water

TABLE 2. Summary of Activation Energy of Barite Reactions

$E_a$ (kcal/mol)	reaction	ref
9.59	dissolution by DTPA	this study
9.31	dissolution by EDTA	this study
10.7	dissolution by DTPA	4
5.9	dissolution by deionized water	11
7.6	dissolution by water (pH = 5.7)	12
6.0	dissolution by deionized water and NaCl	8
5.3	precipitation	8

and the dissolver solvent such as ionic strength and solvation energy. Therefore,  $E_a$  values of barite dissolution done by water only can be used as a reference, not for baseline data of dissolver dissolution. More detailed studies (surface phenomena and kinetics) of barite dissolution by water using atomic force microscopy (AFM) and SEM investigations will be presented elsewhere (25, 26).

The activation energy values obtained in this work are indications of whether either mass transport or surface is the controlling factor. Caldin (18) and Blesa et al. (19) pointed out that the activation energy values below 3.6 kcal/mol indicate a significant contribution from the mass transport kinetics. Activation energies are determined by measurement of bulk scale and may depend on the fraction of faces present on the scale. Data of the activation energies of barite



TABLE 3. Surface Chemical Composition of Barium Sulfate Crystal

element	AEM surface composition (%)	molecular model surface composition (%) <sup>a</sup>
barium (Ba)	59.2	62
oxygen (O)	30.3	34
sulfur (S)	3.8	4
potassium (K)	2.1	
calcium (Ca)	4.6	

<sup>a</sup> Adopted from ref 23.

dissolution by DTPA (9.59 kcal/mol) and EDTA (9.31 kcal/mol) are listed in Table 2. Comparing these data, the activation energy for dissolution of barite is distinctly too high for considering dissolution as a transport-controlled process. Surface control, on the other hand, can be responsible for the detachment of dissolution units from the kink sites, either into the bulk solution or on the surface as the rate-controlling process, and can further be responsible for surface diffusion or desorption from surface as the rate-controlling process (24). Therefore, the surface reaction becomes a significant contribution to the dissolution process in a stirred system.

The strong temperature dependence of the dissolution rate indicates a thermally activated mechanism, with an activation energy consistent with chemical reaction of surface complexes. In a 0.18 M DTPA solution, the dissolution rate of barium sulfate scale is highly temperature dependent with an empirical activation energy of 9.59 kcal/mol. In the same conditions as DTPA, the empirical activation energy of EDTA is about 9.31 kcal/mol. Both values of the activation energy of DTPA and EDTA are too high for the volume diffusion in the solution (3.6 kcal/mol) and suggest surface reaction as the rate-controlling step in the dissolution process. Therefore, the surface reaction is a significant contribution to the dissolution process in a stirred system. Even for a brief analysis of a static system, the activation energies approach that of a stirred system rendering that mass transfer is not important but surface reaction is essential.

**Microanalysis.** The morphology examination by SEM is successful for both dissolution test and crystal growth. The SEM investigations of barite dissolution are shown in Figure 2. Figure 2A presents the SEM micrography of barite before dissolution process showing no pits and cavities on the surface. The examined (001) surface chemical composition (element analysis) of a barite sample was analyzed by Auger electron microscopy (AEM), also shown in Table 3. The (001) surface chemical composition of a barite crystal is similar to the simulation of (001) surface coverage from molecular modeling of the Barite unit cell (23). It is confirmed that the (001) surface of a Barite crystal is the most available surface for reaction. The SEM examination of 0.5 h barium sulfate dissolution by 0.18 M DTPA, illustrated in Figure 2B, shows the initial dissolution dominated in two surfaces with lowest energy: (210) and (001) (13, 15). Those etch pits followed the same direction on the (210) surface. This observation proved the etch pits on the (210) surface started to elongate the crystallographic *b* axis initially. Figure 2C presents the SEM picture of 1 h dissolution of barium sulfate by 0.18 M DTPA. It was very clear that the etch pits followed the same direction, and the average pit size was 2.5  $\mu\text{m}$ . Figure 2D shows the amorphous solid which was the residue of scale dissolved by DTPA in 7 h. The end of the etch pits were terminated by an obtuse angle which formed pronounced cavities. By the SEM observations, the morphology changes and scale dissolution

are considered as a function of dissolution time (26). Surface phenomena are very important to the scale dissolution study. The initial dissolution starts on the two lowest energy surfaces: (001) and (210). The etch pits are elongated in one direction on the specific surface. Surface reaction is essential to scale dissolution according to the kinetics study and microanalysis. It can form etch pits on the specific surface as defect centers.

## Acknowledgments

The authors express their appreciation for a research grant by the Chevron Petroleum Technology Company, La Habra, California, to the University of Southern California. The authors are grateful for all valuable comments made from three reviewers and the editor.

## Literature Cited

- (1) Oddo, J. E.; Tomson, M. B. *SPE Prod. Facil.* **1994**, February, 47–54.
- (2) Benton, W. J.; Collins, I. R.; Grimsey, I. M.; Parkinson, G. M.; Rodger, S. A. *Faraday Discuss.* **1993**, 95, 1–18.
- (3) Haarberg, T.; Selm, I.; Granbakken, D. B.; Fstfold, T.; Read, P.; Schmlidt, T. *SPE Prod. Eng.* **1992**, February, 75–84.
- (4) Putnis, A.; Putnis, C. V.; Paul, J. M. *SPE 29094*, **1995**, February, 773–785.
- (5) Paul, J. M.; Morris, R. L. United States Patent 5,093,020, March 1992.
- (6) Morris, R. L.; Paul, J. M. United States Patent 4,980,077, December 1990.
- (7) Economu, E. D.; Evmiridis, N. P.; Vlessidis, A. G. *Ind. Eng. Chem. Res.* **1996**, 35, 465–474.
- (8) Christy, A. G.; Putnis, A. *Geochim. Cosmochim. Acta* **1993**, 57, 2161–2168.
- (9) Kornicker, W. A.; Presta, P. A.; Paige, C. R.; Johnson, D. M.; Hileman, O. E.; Snodgrass, W. J., Jr. *Geochim. Cosmochim. Acta* **1991**, 55, 3531–3541.
- (10) Liu, S. T.; Nancollas, G. H. *J. Inorg. Nucl. Chem.* **1971**, 33, 2311–2316.
- (11) Bovington, C. H.; Jones, A. L. *Trans. Faraday Soc.* **1970**, 66, 764–768.
- (12) Dove, P. M.; Czank, C. A. *Geochim. Cosmochim. Acta* **1995**, 59, 1907–1915.
- (13) Van Der Leeden, M. C.; Van Rosmalent, G. M. *J. Colloid Interface Sci.* **1995**, 171, 142–149.
- (14) Todd, A. C.; Yuan, M. D. *SPE Prod. Eng.* **1992**, February, 85–92.
- (15) Davey, R. J.; Black, S. N.; Bromley, L. A.; Cottier, D.; Dobbs, B.; Rout, J. E. *Nature* **1991**, 353, 8, 549–550.
- (16) Suito, E.; Takiyama, K. *Proc. Jpn. Acad.* **1952**, 28, 8, 133–138.
- (17) Dunn, K.; Shuler, P. J.; Tang, Y.; Yen, T. F. *Preprint, Div. Petroleum Chem. ACS*, **1997**, 42 (3), 691–693.
- (18) Caldin, E. F. *Fast Reactions in Solution*; Blackwell Scientific: Oxford, 1964.
- (19) Blesa, M. A.; Morando, P. J.; Regazzoni, A. E. *Chemical dissolution of metal oxides*; CRC Press: Boca Raton, FL, 1994.
- (20) Putnis, A.; Junya-Rosso, J. L.; Hochella, M. F., Jr. *Geochim. Cosmochim. Acta* **1995**, 59 (22), 4623–4632.
- (21) Sjöberg, E. L.; Rickard, D. *Geochim. Cosmochim. Acta* **1983**, 47, 2281–2285.
- (22) Söhlne O.; Garside J. *Precipitation, basic principles and industrial applications*; Butterworth-Hienemann Ltd.: Oxford, 1992.
- (23) Blanco, M.; Tang, Y.; Shuler, P.; Goddard, W. A., III. *Mol. Eng.* **1997**, 7, 491–514.
- (24) Jordan, G.; Rammensee, W. *Geochim. Cosmochim. Acta* **1996**, 60, 5055–5062.
- (25) Wang, K. S.; Resch, R.; Dunn, K.; Shuler, P. J.; Tang, Y.; Koel, B. E.; Yen, T. F. *Colloids Surf.* **1999**, in press.
- (26) Dunn, K.; Daniel, E.; Shuler, P. J.; Chen, H. J.; Tang, Y.; Yen, T. F. *J. Colloid Interface Sci.* **1999**, 214.

Received for review September 21, 1998. Revised manuscript received May 24, 1999. Accepted June 8, 1999.

ES980968J